STUDY OF THE RED CORONAL LINE WITH ALTITUDE FROM OUT-OF-ECLIPSE OBSERVATIONS DURING SOLAR CYCLE 24

© 2025 S.A. Guseva*, A.D. Shramko

Kislovodsk Mountain Astronomical Station of Central (Pulkovo) Astronomical Observatory, Russian Academy of Sciences, Kislovodsk, Russia

*svgual@yandex.ru

Received February 14, 2024
Revised March 11, 2024
Accepted March 13, 2024

Abstract. The article presents the results of studies of the emission coronal line λ=6374 Å (FeX) for the period of solar cycle 24. The spectral data were obtained with an out-of-eclipse Lyot coronagraph at the Mountain Astronomical Station of the Pulkovo Observatory, Russian Academy of Sciences (near Kislovodsk). Based on the processing of the results of out-of-eclipse observations, a database of three types of daily coronal maps with a distribution by altitude h from 1 $R_\odot$ to 1.38 $R_\odot$ ($R_\odot$ is the radius of the Sun) of the red line intensity (I_{6374}) was created. Throughout the solar cycle, spectral observations demonstrating a Doppler shift along the red line λ = 6374 Å were found. The extension of the red line from the limb position angle of the Sun was calculated. It was shown that the maximum value of the average extension of the coronal line over the entire limb falls on the ascent branch of solar cycle 24. For different phases of the considered solar cycle (for the ascending branch, the period of maximum, the descending branch and the minimum of solar activity) and for different regions of solar activity, the dependences of the change in I_{6374} values with altitude were plotted and explained. A regression analysis of the obtained relationships is carried out. The regression equations are presented. The changes in I_{6374} with altitude for the polar regions (for all phases of the cycle except for the maximum and the descending branch) and for the middle latitudes (for the minimum of activity) most likely have a logarithmic dependence, and the approximating trend curves for the remaining latitudinal zones are determined by a third-order power function.

Keywords: *solar corona, spectral coronal lines, coronal line intensity*

DOI: 10.31857/S00234206250105e8

INTRODUCTION

Approximately once a year and for only a few minutes (≤7 min), an amazing astronomical event can be observed on Earth — the Sun's corona, which flashes as a silvery-pearly glow during a total solar eclipse. Scientific studies of the solar corona began after the observation of the solar eclipse on July 8, 1842. Later, photographic and spectroscopic methods of analysis were utilized to study the Sun's corona. Observation and study of the solar corona is a crucial task in solar physics. And thanks to the invention in 1930 of the non-eclipse coronagraph by French astronomer B. Lyot (*Fr* . Bernard Lyot) [1], observations of the Sun's corona became possible not only during rare total solar eclipses in the narrow strip of territory where the total phase passes. The application of the Lyot coronagraph system allowed astronomer M . Waldmeier (*Eng.* Max Waldmeier) in 1939 to begin systematic

coronal observations in Switzerland on Mount Arosa [2]. In the same year, German astrophysicist W. Grotrian (*Ger.* Walter Robert Wilhelm Grotrian) proved that the red spectral line, which along with other coronal lines could not be identified for 70 years, belonged to a highly ionized iron atom — FeX [3] with an ionization potential of 233 eV. Thus, it was shown that temperatures of about 10^6 K are required to generate radiation in the coronal lines [4]. The red line $\lambda = 6374$ Å is not as bright as the green $\lambda = 5303$ Å (FeXIV), and, unfortunately, not all observatories included this line in their observation programs. Continuous observations of the line $\lambda = 6374$ Å were conducted at the following observatories: in Switzerland (1939 yr.) — Arosa (*Ger.* Arosa), in France (1947 yr.) — Pic du Midi (*Fr* . Pic du Midi), in the USA (1949 yr.) — Sacramento Peak (*Eng.* Sacramento Peak), in the USSR (1952 yr.) — MAS MAO RAS [5], in Czechoslovakia (1964 yr.) — Lomnický Štít (*Slovak.* Lomnický štít). Despite the fact that the worldwide network of coronal stations created in the 20th century ceased to exist, the study of the spectral corona is still relevant today. The solar corona is the source of the solar wind, and regular observations of changes in coronal line intensity by position angle and height allow for a deeper understanding of the patterns of solar activity and its effect on space weather. The study of forbidden coronal line intensities is of great interest for understanding the physical processes occurring in the solar atmosphere and for predicting changes in geomagnetic and solar activity (SA). According to the unified international methodology for processing coronal lines, which was proposed by M.N. Gnevyshev [6], the line intensity is measured at a specific height $h = 1.04$ $R_\odot$. This methodology for processing spectral corona data at the Mountain Astronomical Station GAO RAS is observed to this day, while other observatories in their final years of observations stopped following it. For instance, the Lomnický Štít observatory conducted measurements of I_{6374} at $h = 1.06$ $R_\odot$, and Sacramento Peak at $h = 1.15$ $R_\odot$. The peculiarities of the distribution of I_{6374} along the limb at other heights from the solar photosphere were not included in the " Solar Service," and therefore fewer such studies were conducted, especially over extended periods of time [7–16]. Often such research was carried out using spectral data obtained during solar eclipses [11, 13].

Previously, the authors conducted a study of the radial distribution of the coronal line $\lambda = 6374$Å during the minimum of SA [17]. For 2009, curves of the red line intensity changes at different heights from the solar limb were obtained for polar, mid-latitude, and equatorial regions. The work was continued for an entire solar cycle.

The purpose of this study is to investigate changes in the parameters of the coronal line $\lambda = 6374$ Å with height from 1 $R_\odot$ to 1.38 $R_\odot$ using extensive observational data.

OBSERVATIONAL DATA

This work uses spectral data of the red coronal line $\lambda = 6374$ Å (FeX), obtained during the 24th solar activity cycle using the Lyot non-eclipse coronagraph at the Mountain Astronomical Station of the GAO RAS [18]. During this period (2010–2019), there were on average 180 gg.) on average per year of coronal observations there were 180 days of coronal observations per year. It should be noted that the 24th solar activity cycle had the highest number of coronal observation days compared to other solar activity cycles [18]. Digital cameras Canon EOS 450D and 600D were used to photograph the corona spectrum. As a result of processing, in accordance with the " Solar Service" program, the intensities of coronal lines (I_{5303} and I_{6374}) are calculated in absolute units (abs. units), expressed in millionths of the energy contained in a 1 Å wide interval of the continuous spectrum of the Sun's center, measured at a distance of 40 ″ from the Sun's photosphere 6]. Figure 1 shows the time series of the 24th cycle spectral corona I_{6374} (abs. units) according to these data. Spectral observations at the Mountain Astronomical Station of GAO RAS allow measurements of I_{6374} along the line up to a height of 6 ′ (1.38 $R_\odot$).

Fig. 1. Changes in the intensity of the coronal line λ = 6374 Å (FeX) during the 24th solar activity cycle. The thin line shows daily values of I_{6374} (abs. units) averaged over the entire limb, and the thick line shows their monthly averages.

PRELIMINARY ANALYSIS OF CORONAL SPECTRA

Over 10 years, 1822 days of red spectral corona observations were processed. The total number of processed frames was 131,184. Analysis of digital photographs showed that, as in the green spectral region [19-20], there are days in the red spectrum where intense emissions are observed in several lines. M.N. Gnevyshev called this phenomenon coronal activity impulses. These coronal activity impulses are accompanied by eruptive prominences, such as *eng.* surges, in which rapid changes and intense movements are observed. Most of them are associated with flares. In Fig. 2a shows the emission spectrum of such an eruptive prominence in the Hα line (λ = 6563 Å) and in the emission line of the Mg triplet (λ = 5167 Å, λ = 5173 Å, λ = 5184 Å) from 14.III.2014, where the green spectrum was observed at 9:42, and the red one at 9:36 UT. Such transient events on the Sun are rare and difficult to capture, they are characterized by a wide range of spatial and temporal scales - from eruptive prominences to coronal mass ejections (*Eng.* CME - Coronal Mass Ejection). As an example, Fig. 2b shows the spectrum in the red emission range in several lines from 30.X.2014. Previously [19] for this date, a spectrum with pulses of coronal activity in the green wavelength range was presented. Fig. 2b captures a rare moment when the emission of the coronal line λ = 6374 Å and chromospheric lines Hα (λ = 6563 Å), and BaII (λ = 6497 Å) are simultaneously visible. During a solar flare or coronal mass ejection on the Sun, intense radiation occurs in a wide range of wavelengths, including both the visible spectrum region and ultraviolet, X-ray, and radio ranges. During such transient events on the Sun, spectral lines can have different intensities and profiles, so their parameters and properties can change depending on the characteristics and intensity of the flare or ejection. The coronal line λ = 6374 Å, like the line λ = 5303 Å [19] during the emission of such pulses of coronal activity has a heterogeneous structure along the line (Fig. 2a-b) .

Fig. 2. Panel a - examples of heterogeneous coronal line λ = 6374 Å during emission of eruptive "surge" type prominence in Hα line (λ = 6563 Å) and in the emission line of Mg triplet λ = 5167 Å, λ = 5173 Å, λ = 5184 Å). The date and position angle are indicated; panel b - example of spectrum with emission in coronal line λ = 6374 Å, Hα (λ = 6563 Å) and Ba (λ = 6497 Å), where 125 ° is the position angle; panel c - examples of heterogeneities along the coronal line λ = 6374 Å above active regions near the limb.

Heterogeneous structure along the red line is observed more frequently than in the green line (Fig. 2c). Unlike the green line, where there are several bright clumps that resemble grains strung along this line [19], inhomogeneities along the red line have a different appearance. At the base, the red line is bright and wide, and then it sharply loses intensity. It may widen even more. There is a strong asymmetry of the line, shifts are observed in one direction and another along the line, such Doppler shifts of the line λ = 6374 Å were obtained and described by the author during the observation of the solar eclipse on 29.III.2006 [11]. The spectral frames of the red line obtained during the eclipse were observed over the active region, where the height of the spectrum in one frame covered the area from 1 $R_\odot$ to 1.5 $R_\odot$, and in another frame from 1.02 $R_\odot$ to 1.86 $R_\odot$ from the visible center of the Sun. When a sunspot group is at the limb of the Sun, a relatively large bright clump may be present in the middle of the red coronal line. Or similarly, as for the green line, several

bright clumps, but they are not clearly defined; there are fewer such observations than in the green spectrum [19]. Apparently, the inhomogeneities along the red and green lines have different natures. The radiation of the red spectral corona occurs predominantly in regions with open magnetic field (MF) structures, while the green corona in the line $\lambda = 5303$ Å is emitted by structures in which active regions and associated closed MF configurations (coronal loops) dominate, and is responsible for hotter plasma [7-9]. The red line $\lambda = 6374$ Å is emitted from cooler plasma, which is present in almost the entire solar corona, including coronal holes.

METHODS AND RESULTS OF PROCESSING OF THE RED CORONAL LINE

Catalogs of daily coronal maps

Using the IDL6.1 package (*English.* Interactive Data Language) a computer program was written to process spectral coronal data of the red line $\lambda = 6374$ Å. Calculations of I_{6374} were conducted from the limb, starting from a height of $h = 2''$ and with a step of 2.5 ″ along the line to the end of the frame. The height of the spectrum in the frames varies from 320 ″ to 500 ″ depending on the positional angle. Frames with the smallest spectrum height cover only the polar latitudes of the Sun. As a result of processing non-eclipse coronal observations, a database of three types of daily coronal maps with I_{6374} at a height from 1 $R_\odot$ to 1.32 $R_\odot$ was created:

- maps with plotted isolines of I_{6374} values at different heights from the solar limb (Fig. 3a);
- maps showing the change with height of I_{6374} values in the form of grayscale gradation (Fig. 3b);
- 3D-maps of I_{6374} at a specific height (Fig. 3c). These 3D-maps display I_{6374} values for all days observed within the given half-rotation of the Sun. For comparison, 3D-maps of the spectral corona intensity at a height of $h = 40''$ (Fig. 3c) are presented.

Fig. 3. Examples of daily coronal maps of the spectral corona with I_{6374} at a height of h (1–1.32) $R_\odot$: a — maps with plotted isolines of I_{6374} values at different heights from the solar limb; b — maps showing the distribution of I_{6374} values with height, in the form of grayscale gradation (in inversion); c — 3D-maps of I_{6374} spectral corona at a specific height, where $h = 40''$.

Fig. 3 shows examples of daily coronal maps during the rising branch, maximum, and declining branch of the 24th solar activity cycle, where days with different spectral corona configurations were selected. For clarity, different types of maps are shown for the same day. On these maps (Fig. 3a) it is seen that in most cases up to a height $h = 70''$ the isolines of I_{6374} can change their configuration with height. The lower the height, the greater the chaos of the isolines. Just as on maps for I_{5303} [19], there is a shift in the maximum of isolines I_{6374}, but it is not as distinct and occurs less frequently. For example, on the map from 2.II.2010 in the SW *(English:* Southwest) quadrant up to $h = 100''$, although the maximum has small jumps, it is closer to the pole, and then it deviates 10° toward the equator. In [21], the deviation from the radial direction of coronal rays in white light was investigated depending on the phase of the solar activity cycle, using data from the wide-angle coronagraph LASCO C2 (*English:* Large Angle and Spectrometric Coronagraph) of the space observatory *SOHO* (*English . Solar and Heliospheric Observatory*). As with coronal rays in white light, the intensity maxima of the spectral line $\lambda = 6374$Å at different heights ("red rays") have deviations in the direction of higher or lower latitudes. Thus, the constructed maps clearly show the deviation of the "red ray" with height from the radial direction, but large inclination angles up to 25–35°, as for coronal rays in white light [21], are not observed.

Inhomogeneities along the line are clearly visible on the maps in Fig. 3b. Analysis of catalogs of daily coronal maps (Fig. 3) showed that at the beginning of the 24th solar activity cycle, the values of I_{6374}, as well as for I_{5303}, predominate in the northern hemisphere of the Sun, that is, there is an asymmetry in the appearance of active regions (AR) in favor of the northern hemisphere. The same asymmetry is observed in the areas of sunspots (http://solarstation.ru).

Extension of the coronal line

For the 24th solar activity cycle, changes in the extension of the coronal line from the positional angle of the Sun were considered. The line extension was calculated taking into account the halo for a given day. The temporal distribution of the line extension values λ = 6374 Å (FeX) around the entire limb for the 24th solar activity cycle differs significantly from the similar distribution for the line λ = 5303 Å (FeXIV) [19]. The maximum values of the average extension h_{avg} of the coronal line around the entire limb occur during the period 2010-2011 yrs. (Fig. 4a). To account for the activity level of different latitudinal regions, the solar limb was divided into the following zones: 1st — equatorial: ±30° from the equator; 2nd — middle latitudes: from ±30° to ±60°; 3rd — polar: 30° from the poles of the Sun.

Fig. 4. Graphs showing the dynamics of the extension of the coronal line λ = 6374 Å (FeX) during the 24th solar activity cycle: a — changes in the values of maximum h_{max} and average h_{avg} line extension around the entire limb; b — variations in the average extension h_{avg} of the line above certain latitudinal zones of solar activity: 1 — equatorial; 2 — middle; 3 — polar.

Above the equatorial regions (1st zone) and above the middle latitudes (2nd zone), the coronal line reaches its maximum height during the rising phase of the solar cycle (Fig. 4b). In Fig. 4b, it is clearly visible that at the beginning of the cycle, the coronal activity of middle latitudes dominates, the extension of the line h_{avg} of the 2nd zone is higher than h_{avg} of the 1st zone, and during the maximum period, the coronal activity of equatorial latitudes prevails; on the declining branch and until the end of the cycle, the extension h_{avg} of these two zones is comparable. In the polar regions (3rd zone), the emission of the coronal line reaches its maximum height during the period 2010-2011 yrs., and its second maximum in 2013 yr. (Fig. 4b). The distribution of the extension of the red line in polar latitudes precedes by one year the latitudinal drift of the neutral line dividing the polarity of the Sun's magnetic field. According to synoptic Hα-maps constructed from the data of GAS GAO RAS M.P. According to Fatyanov (http://solarstation.ru), the polar magnetic field reversal in the northern hemisphere of the Sun occurred from late 2012 to mid-2013 . And for almost a year, both poles of the Sun had positive polarity. From September 2014 , the polarity reversal process occurred at the southern pole of the Sun. Another maximum of h_{avg} for the 3rd zone is observed in mid-2016 . Thus, in the polar regions, we observe red line activity in antiphase with the green line. In the latitudinal distribution of the emission corona during the 22nd and 23rd solar activity cycles, a similar decrease in the intensity values of the red corona at the pole was observed, comparable to the green corona [15]. During the maximum of the solar activity cycle, the fluctuations in corona intensity in these lines show antiphase changes.

Change in the intensity of the line λ = 6374Å with height

To account for variations of I_{6374} depending on the activity level of a given region, graphs of the intensity distribution of the line λ = 6374Å with height were constructed separately for each of the three zones. These curves averaged over the entire 24th cycle are shown in Fig. 5a. For a more

detailed study, the calculation of I_{6374} with height was carried out separately for the rising phase, maximum, declining phase, and minimum of solar activity (Fig. 5b).

Fig. 5. Change with height h of the intensity of the line λ 6374Å during the 24th solar activity cycle: a — dependence of I_{6374} for different latitudinal zones of the solar limb: 1 — equatorial; 2 — middle; 3 — polar; 4 — the entire limb of the Sun; b — distribution of I_{6374} separately for the rising branch (↗) and declining branch (↘), maximum (max) and minimum (min) phases of the solar activity cycle, where the numbers indicate the latitudinal zone.

Approximating curves for the 1st zone have the following form:

$$I_{\uparrow} = 26.6 - 0.3h + h^2 - 2\cdot10^{-6}h^3, \sigma = 10.1, \quad (1)$$

$$I_{max} = 24.4 - 0.2h + h^2 - 1.7\cdot10^{-6}h^3, \sigma = 13.5, \quad (2)$$

$$I_{\downarrow} = 21 - 0.2h + h^2 - 1.3\cdot10^{-6}h^3, \sigma = 6.2, \quad (3)$$

$$I_{min} = 15.2 - 0.1h + h^2 - 9\cdot10^{-7}h^3, \sigma = 3.7, \quad (4)$$

where $I_{\uparrow}$ — values of I_{6374} on the rising branch of the SA; I_{max} — intensity of I_{6374} at the maximum of SA; $I_{\downarrow}$ — values of I_{6374} on the declining branch of SA; I_{min} — I_{6374} at the minimum of SA; σ — standard deviation.

The highest values of I_{6374} at all heights h are observed on the curve of the rising branch of the cycle ($I_{\uparrow}$). Unlike the green line, where the distribution of I_{5303} at all heights h was dominated by the curve I_{max} [19]. The values of I_{6374} on the curve $I_{\uparrow}$ decrease up to $h = 150''$, and the curve I_{min} also changes up to this height. And during the maximum phase (I_{max}) the curve I_{6374} has the steepest and most prolonged decline, and at large heights $h \geq 130''$, the lowest values of I_{6374} are observed compared to other phases of SA. At the height $h = 70''$, the curve $I_{\downarrow}$ is higher than I_{max}. The rising branch of the activity cycle ($I_{\uparrow}$) and the declining branch ($I_{\downarrow}$) have a greater height gradient than the curve I_{min}. And the curve I_{min} at high altitudes has the following feature: at $h = 130''$ it intersects I_{max} and then goes above it, and from the height $h = 220''$, the curve I_{min} is comparable with $I_{\downarrow}$ (Fig. 5b).

Approximating curves for the 2nd zone:

$$I_{\uparrow} = 18.2 - 0.1h + h^2 - 1.4\cdot10^{-7}h^3, \sigma = 9.7, \quad (5)$$

$$I_{max} = 15.5 - 0.2h + h^2 - 1.8\cdot10^{-7}h^3, \sigma = 14.9, \quad (6)$$

$$I_{\downarrow} = 15.6 - 0.1h + h^2 - 1.3\cdot10^{-6}h^3, \sigma = 8, \quad (7)$$

$$I_{min} = 14.5 - 3.27Lg(h) + 0.1Lg^2(h), \sigma = 5.4. \quad (8)$$

For the 2nd zone, as for the 1st one, the highest values of I_{6374} are characteristic for the rising branch of the cycle ($I_{\uparrow}$), both for small and large heights. The lowest values of I_{6374} are observed at heights $h > 50''$ at the maximum of SA (I_{max}), the curve I_{max} lies even below I_{min} (Fig. 5b).

Approximating curves for the 3rd zone:

$$I_{\uparrow} = 14.6 - 2.8Lg(h) + 0.4Lg^2(h), \sigma = 3.3, \quad (9)$$

$$I_{max} = 16.6 - 0.2h + h^2 - 2\cdot10^{-6}h^3, \sigma = 17.1, \quad (10)$$

$$I_{\downarrow} = 16.2 - 0.2h + h^2 - 1.5 \cdot 10^{-6} h^3, \quad \sigma = 9.8, \qquad (11)$$

$$I_{\min} = 11.8 - 1.3Lg(h) - 0.2Lg^2(h), \quad \sigma = 1.5. \qquad (12)$$

In polar latitudes, the highest values of I_{6374} at low heights ($h < 50''$) correspond to the phases of maximum ($I_{\max}$) and decline ($I_{\downarrow}$) of the SA cycle. And the highest values of I_{6374} at heights $h > 50''$ belong to the rising branch of the solar cycle ($I_{\uparrow}$).

Equations of the average approximating curves for the 24th SA cycle:

$$I_{24цикл} = 17.1 - 0.1h + h^2 - 1.3 \cdot 10^{-6} h^3, \quad \sigma = 4.3, \qquad (13)$$

$$I_1 = 20.8 - 0.2h + h^2 - 1.4 \cdot 10^{-6} h^3, \quad \sigma = 5.2, \qquad (14)$$

$$I_2 = 14.7 - 0.1h + h^2 - 1.2 \cdot 10^{-6} h^3, \quad \sigma = 7.1, \qquad (15)$$

$$I_3 = 13.7 - 0.1h + h^2 - 1.1 \cdot 10^{-6} h^3, \quad \sigma = 4.6, \qquad (16)$$

where $I_{24\,\text{cycle}}$ is the intensity of the line $\lambda = 6374$ Å averaged over all latitudes for the entire 24th SA cycle; I_1, I_2, I_3 are the averaged intensity of the red line in the corresponding latitudinal zone (Fig. 5a). For I_{6374} there is deviation I_1 from I_3 only within 6 abs. units, unlike I_{5303}, where the difference between these values was 46 abs. units [19]. The curves of averaged values I_{6374} for the entire cycle for different regions decrease at different rates up to a height of 200″, and at $h > 200''$ the curves I_1, I_2, I_3 converge. Unlike I_{5303}, where the curves I_1, I_2, I_3 continue to decrease above a height of 300″. At greater heights, there is an increase in the intensity of the red corona compared to the green corona. For example, $I_{24\text{cycle}}$ at a height of $h = 300''$ the values of $I_{6374} = 7.5$ abs. units, while I_{5303} at the same height has values of 3.5 abs. units. If at low heights the red corona is much less intense than the green one, at greater heights the situation changes. This is another difference between I_{6374} and I_{5303} showing that these lines are responsible for different nature of radiation — closed and open MP.

CONCLUSION

The red coronal line $\lambda = 6374$ Å (FeX) is the second most intense emission of all coronal emission lines in the optical range after the green line $\lambda = 5303$ Å (FeXIV) and is also observed at all position angles of the solar limb during the SA cycle. The registration of coronal observations in the 24th SA cycle was completely digital. This made it possible to apply computer image processing methods, which allowed a more detailed study of the structure of coronal spectral lines [18]. As a result of the study of the emission coronal line $\lambda = 6374$ Å for the period of the 24th SA cycle, it was shown that here, as with $\lambda = 5303$ Å, a heterogeneous structure of the line can be observed. The heterogeneity along the red line, although not as pronounced as in the green line, occurs more frequently and not only in the presence of AO. The constructed catalogs of three types of daily coronal maps complement each other well for studying the distribution of I_{6374}, they clearly show a small shift of the I_{6374} maxima in the positional angle with height (the inclination angle of the "red ray"). The analysis of the coronal line extent at different SA phases showed that the distributions of maximum extent ($h_{\max}$) in the 1st and 2nd zones have a similar temporal course and, as a rule, exceed the height of the line in the polar zones. The temporal distribution of the average extent (h_{avg}) of the red line in the 3rd zone precedes by one year the latitudinal drift of the neutral line of the Sun's MP polarity division. Thus, in the polar regions, one can see the radiation of the red line in antiphase with the green line.

The obtained distribution of I_{6374} with height for different phases of the SA cycle is presented. For equatorial and middle latitudes (except for $I_{\min}$), polynomial equations of the third order were determined as approximating curves, while for polar regions (except for $I_{\max}$ and $I_{\downarrow}$)—logarithmic equations. The highest values of I_{6374} at all heights h are shown by the curve on the rising branch of the 24th cycle ($I_{\uparrow}$) for the 1st zone. At heights $h > 100''$ the curves $I_{\uparrow}$ for all three zones under

consideration have the highest values of I_{6374} compared to other phases of the SA cycle. This differs from the green corona, where the constructed curves of I_{5303} for the maximum phase exceed the curves for all other phases of the SA cycle. The curves of averaged values of I_{6374} over the entire cycle for different regions do not have such significant deviations from each other (~ 6 abs. units), as similarly constructed curves for I_{5303}, where the difference between I_1 and I_3 was 46 abs. units [19]. While at low altitudes the red corona's intensity is much lower than the green one, at higher altitudes the red corona's intensity is several abs. units higher compared to the green corona.

Coronal lines observed under the " Solar Service" program can be used to study physical processes in the solar corona, such as heating and temperature distribution, gas and magnetic field movements, as well as to investigate phenomena related to SA, such as coronal mass ejections and solar flares.

REFERENCES

1. *Lyot B.* Étude de la couronne solaire en dehors des éclipses // Z. Astrophys. 1932. V. 5. P. 73-95.
2. *Waldmeier M.* Die Sonnenkorona. V. 2. Basel: Birkhauser, 1957. 353 p.
3. *Grotrian W.* Zur Frage der deutung der Linien in Spectrum der Sonnenkorona // Naturwissenschaften . 1939. V. 27. Iss. 13. P. 214 - 214 .
4. *Shklovsky I.S.* Physics of the Solar Corona. 2nd ed. Moscow: State Publishing House of Physical and Mathematical Literature, 1962. 516 p.
5. *Gnevyshev M.N., Gnevysheva R.S.* The beginning of regular observations of the solar corona outside eclipses // Bull. Commission for Solar Research. 1954. No. 10. P. 60 - 62.
6 . *Gnevyshev M.N.* Technique and methodology of coronal observations // Bull. International Geophysical Year . 1959. P. 36-38.
7. *Tyagun N.F.* Studies of the relationship between half-width and intensity for coronal emission lines FeXIV 5303, FeX 6374 and CaXV 5694 depending on height // Solar-Terrestrial Physics. 2004. No. 6. P. 104-105.
8. *Tyagun N.F.* A symmetry of coronal line profiles FeX λ6374 Å // Solar-Terrestrial Physics. 2009. No. 14. P. 19-22.
9. *Tyagun N.F.* Line widths and Doppler velocities according to the Fe X λ6374 and Fe XIV λ5303 observations performed with the Large Coronograph at Sayan Observatory // Geomagnetism and Aeronomy. 2014. V. 54. Iss. 7. P. 959 – 964.
10. *Delone A.B., Makarova E.A.* Study of red coronal line 6374A contours using interferograms obtained during the solar eclipse on March 7, 1970 // Astron. Circular. 1973. No. 772. P. 1-2.
11. *Guseva S.A., Kim Gun-Der, Tlatov A.G.,* Results of observing the total solar eclipse on 29.03.2006 in coronal line λ6374Å at Kislovodsk Mountain Station // Proc. conf. "Physical nature of solar activity and forecasting its geophysical manifestations". SPb.: MAO RAS, 2007. P. 121-126.
12. *Tyagun N.F., Stepanov V.E.* Latitudinal distribution of total emission and half-width of coronal line Fe X 6374Å // Solar Data. 1975. No. 2. P. 56-64.
13. *Singh J., Bappu M.K.V., Saxena A.K.* Eclipse observations of coronal emission lines. I. [Fe X] 6374Å profiles at the eclipse of 16 February 1980 // J. Astrophys. 1982. V. 3 **.** P. 249-266.
14. *Singh J., Ichimoto K., Imai H., Sakurai T. et al.* Spectroscopic Studies of the solar corona I. Spatial variations in line parameters of green and red coronal lines // Publ. Astronomical Soc. Japan. 1999. V. 51. P. 269-273.
15. Long-term cyclic changes in solar corona structure: abstract of dissertation ... Candidate of Physical and Mathematical Sciences: 01.03.03 / Guseva Svetlana Aleksandrovna; [Defense location: Main Astronomical Observatory RAS]. - Saint Petersburg, 2013. - 22 p.
16. *Singh J., Sakurai T., Ichimoto K. et al.* Spectroscopic Studies of the Solar Corona II. Proprieties of Green and Red Emission Lines in Open and Closed Coronal Structure // Publ. Astronomical Soc. Japan. 2002. V. 54. P. 793-806.

17. *Guseva S.A., Shramko A.D.* Investigation of coronal line 6374Å during solar activity minimum // Proc. conf. "Year of Astronomy: Solar and Solar-Terrestrial Physics-2009". SPb.: MAO RAS, 2009. P. 147-148.
18. *Guseva S.A.* Continuous 60-Year Observations of the Spectral Solar Corona at the Mountain Astronomical Station of Pulkovo Observatory // Geomagnetism and Aeronomy. 2019. V. 59. № 7. P. 864–869.
19. *Guseva S.A.* , *Shramko A.D.* Study of the green coronal line with height based on non-eclipse observations during the 24th solar activity cycle // Cosmic Research. 2023. V. 61. № 2. P. 124–133.
20. *Kim Gun-der* Coronal Activity Impulses // Proc. conf. "Solar Activity as a Space Weather Factor". SPb.: GAO RAS., 2005. P. 403–404.
21. *Guseva S.A., Fatyanov M.P., Shramko A.D.* Configuration of the heliospheric current sheet based on synoptic maps of coronal rays for the 23rd, 24th solar activity cycles // Geomagnetism and Aeronomy. 2015. V. 55. № 3. P. 302–309.

Figure Captions

Fig. 1. Variation in the intensity of the coronal line λ = 6374 Å (FeX) during the 24th SA cycle. The thin line shows daily values of I_{6374} (abs. units) averaged over the entire limb, and the thick line shows their monthly averages.

Fig. 2. Panel a — examples of inhomogeneous coronal line λ = 6374 Å during the emission of surge-type eruptive prominence in Hα line (λ = 6563 Å) and in the emission line of Mg triplet λ = 5167 Å, λ = 5173 Å, λ = 5184 Å). Date and position angle are indicated; panel b — example of spectrum with emission in coronal line λ = 6374 Å, Hα (λ = 6563 Å) and Ba (λ = 6497 Å), where 125 ° is the position angle; panel c — examples of inhomogeneities along the coronal line λ = 6374 Å above active regions near the limb.

Fig. 3. Examples of daily coronal maps of the spectral corona with I_{6374} at height h (1-1.32) $R_{\odot}$: a - maps with plotted isolines of I_{6374} values at different heights from the solar limb; b - maps showing the distribution of I_{6374} values with height, in grayscale (inverted); c - 3D maps of I_{6374} spectral corona at a specific height, where h = 40".

Fig. 4. Graphs showing the dynamics of the coronal line λ = 6374 Å (FeX) extent during the 24th SA cycle: a - changes in maximum h_{max} and average h_{avg} line extent along the entire limb; b - variations in average extent h_{avg} of the line above specific latitudinal SA zones: 1 - equatorial; 2 - middle; 3 - polar.

Fig. 5. Change with height h of line intensity λ 6374Å during the 24th SA cycle: a - dependence of I_{6374} for different latitudinal zones of the solar limb: 1 - equatorial; 2 - middle; 3 - polar; 4 - entire solar limb; b - distribution of I_{6374} separately for the ascending (↗) and descending (↘) branches, maximum (max) and minimum (min) phases of the SA cycle, where numbers indicate the latitudinal zone.

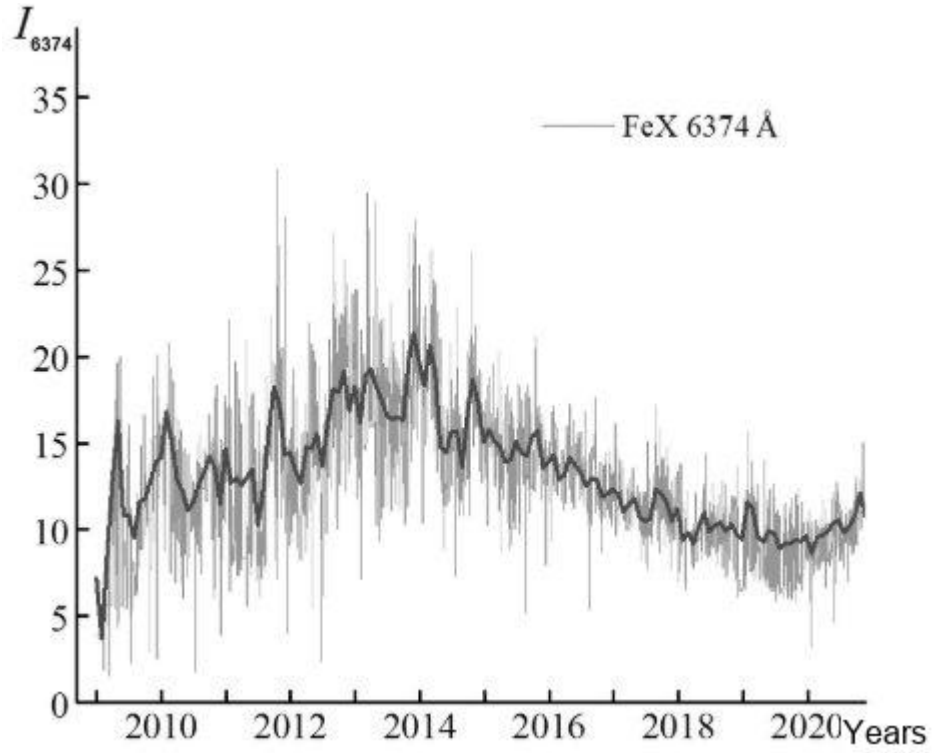
I_{6374}
35
30
25
20
15
10
5
0
FeX 6374 Å
2010
2012
2014
2016
2018
2020
Years

Fig. 1.

(a)

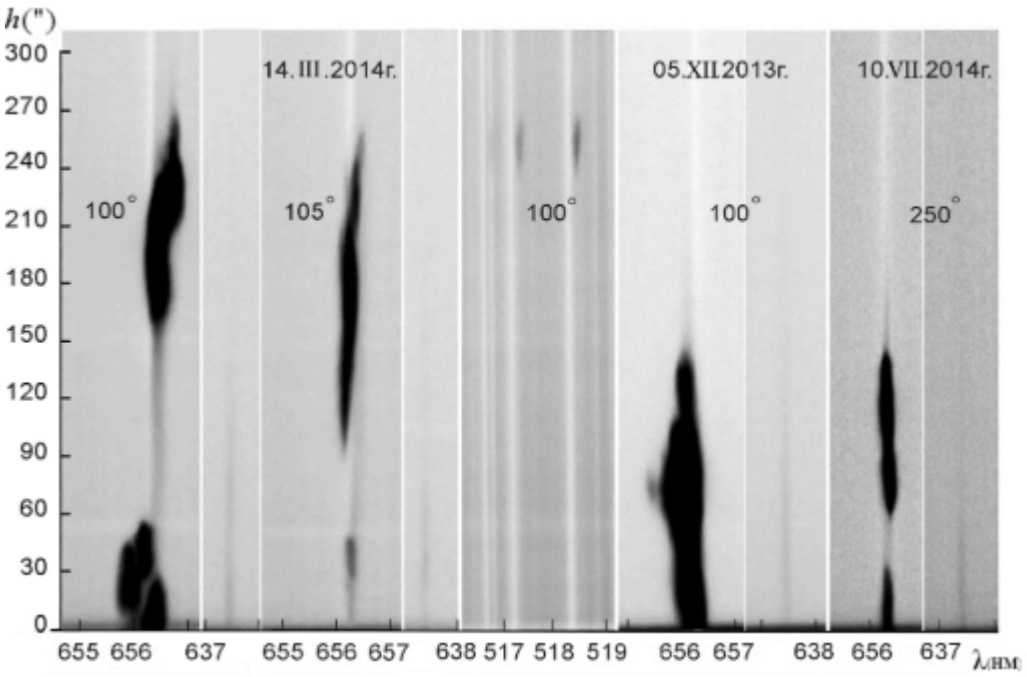
h(")
300
270
240
210
180
150
120
90
60
30
0
14.III.2014r.
05.XII.2013r.
10.VII.2014r.
100°
105°
100°
100°
250°
655 656 637 655 656 657 638 517 518 519 656 657 638 656 637
λ,нм

(b)

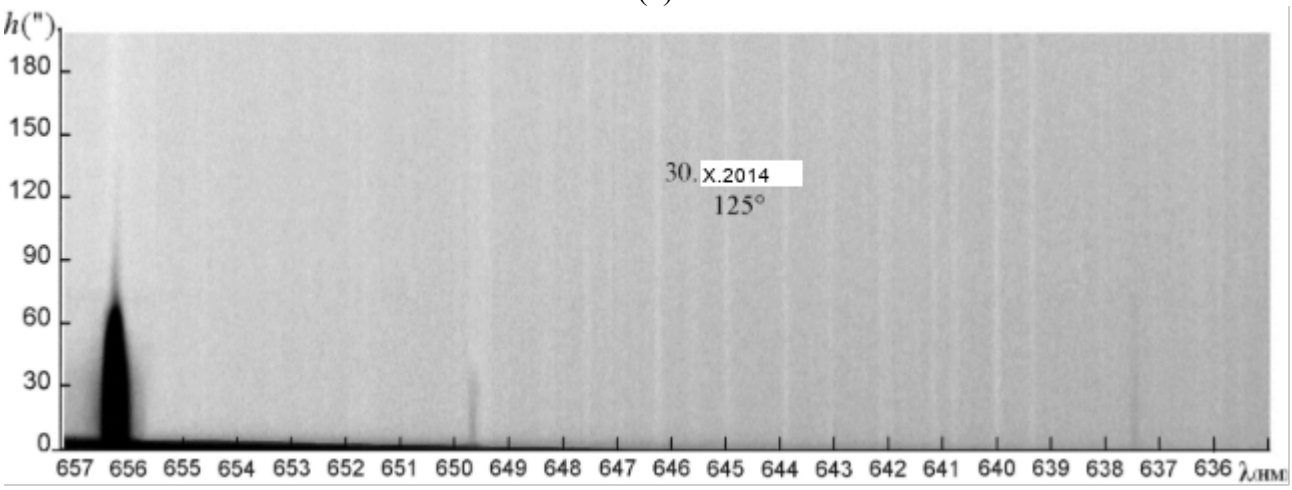
h(")
180
150
120
90
60
30
0
30.X.2014
125°
657 656 655 654 653 652 651 650 649 648 647 646 645 644 643 642 641 640 639 638 637 636
λ,нм

(c)

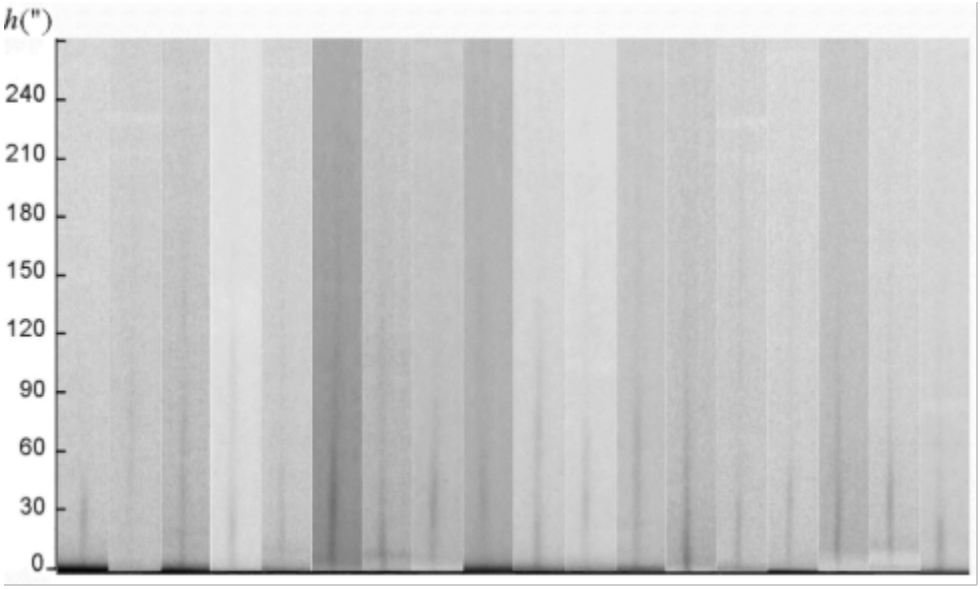

Fig. 2.

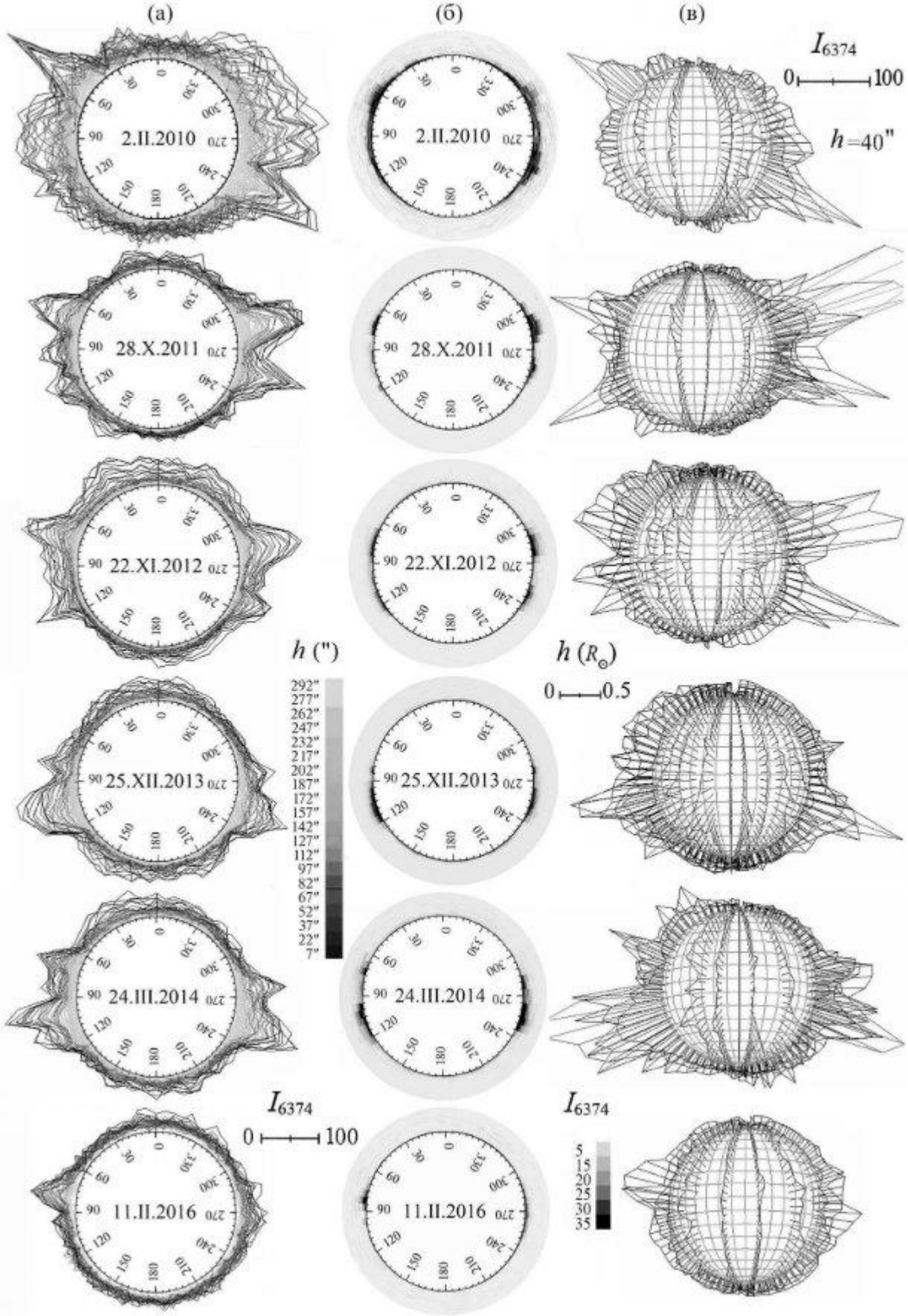
(а)
(б)
(в)
I_{6374}
0 100
h=40"
2.II.2010
28.X.2011
22.XI.2012
25.XII.2013
24.III.2014
11.II.2016
h (")
292"
277"
262"
247"
232"
217"
202"
187"
172"
157"
142"
127"
112"
97"
82"
67"
52"
37"
22"
7"
h ($R_\odot$)
0 0.5
I_{6374}
0 100
I_{6374}
5
15
20
25
30
35

Fig. 3.

(a)

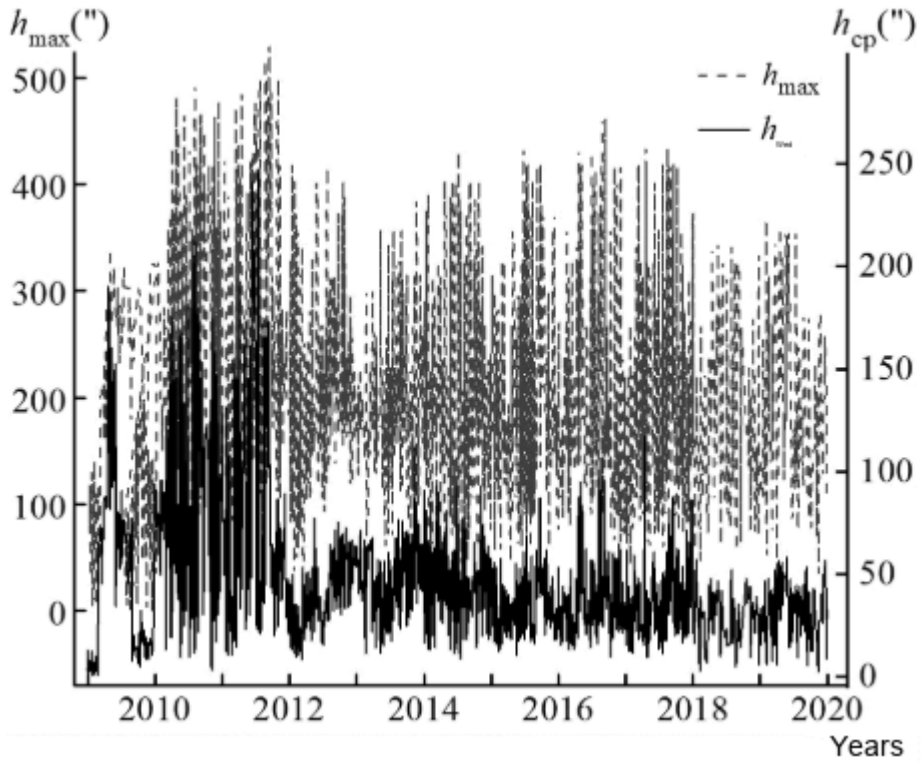
h_{max}(")
h_{cp}(")
500
400
300
200
100
0
250
200
150
100
50
0
h_{max}
2010
2012
2014
2016
2018
2020
Years

(b)

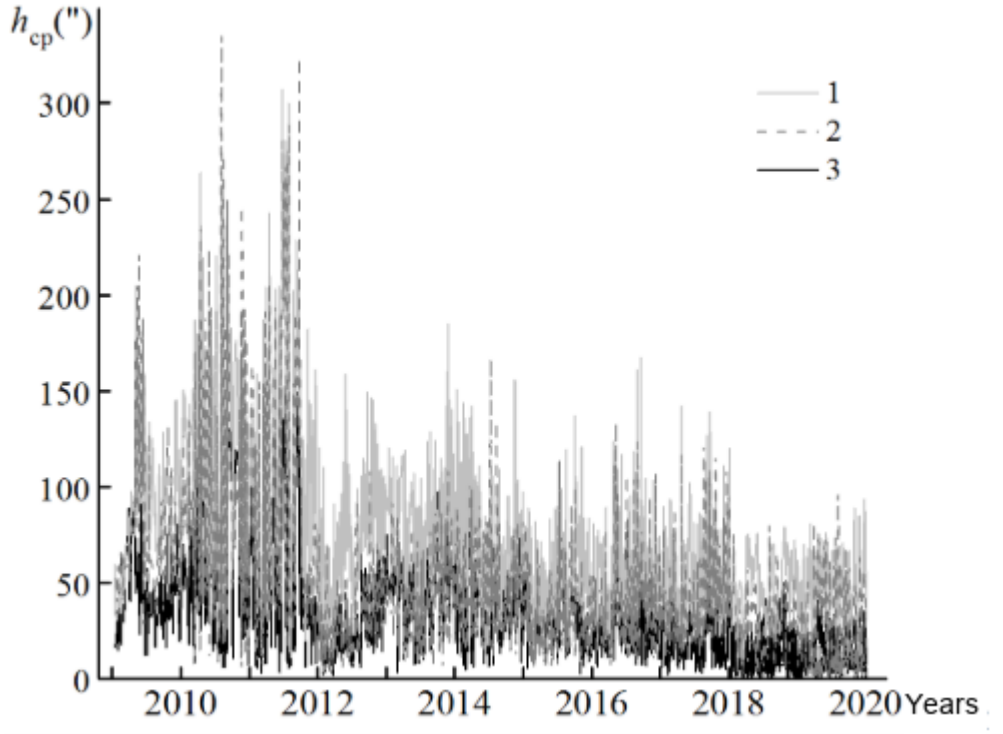
h_{cp}(")
300
250
200
150
100
50
0
1
2
3
2010
2012
2014
2016
2018
2020
Years

Fig. 4.

(a)

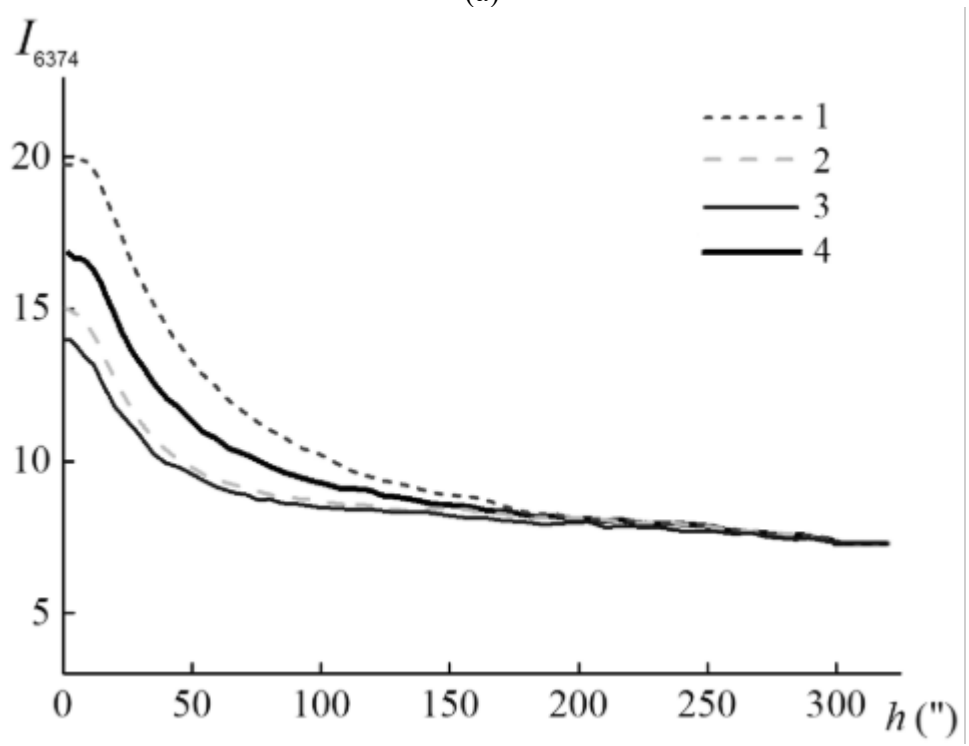
I_{6374}
20
15
10
5
0
50
100
150
200
250
300
h (")
1
2
3
4

(b)

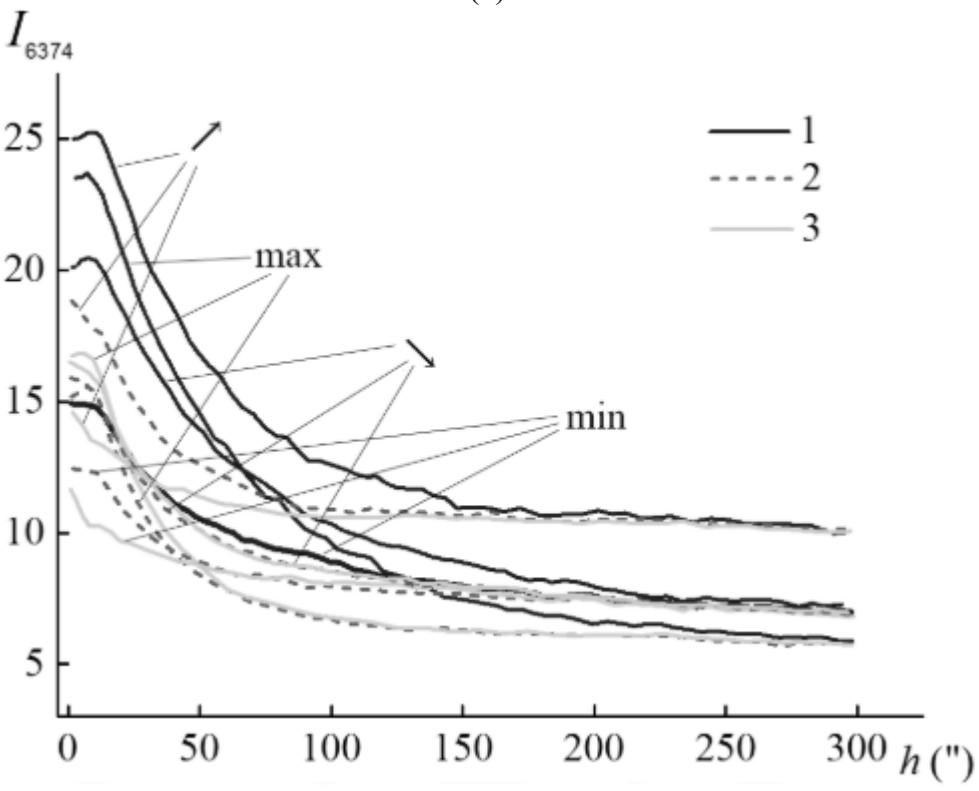
I_{6374}
25
20
15
10
5
0
50
100
150
200
250
300
h (")
max
min
1
2
3

Fig. 5.